CHEMISTRY OF MATERIALS
Article

Chem. Mater. **2010,** *22,* 5013–5021 5013
DOI:10.1021/cm101290f

New Hydrides REScSiH and REScGeH (RE = La, Ce): Structure, Magnetism, and Chemical Bonding

Bernard Chevalier,*,† Wilfried Hermes,‡ Birgit Heying,‡ Ute Ch. Rodewald,‡ Adrienne Hammerschmidt,‡ Samir F. Matar,† Etienne Gaudin,† and Rainer Pöttgen‡

†*CNRS, Université de Bordeaux, ICMCB, 87 Avenue du Docteur Albert Schweitzer, 33608 Pessac Cedex, France, and* ‡*Institut für Anorganische und Analytische Chemie and NRW Graduate School of Chemistry, Universität Münster, Corrensstrasse 30, 48149 Münster, Germany*

Received May 7, 2010. Revised Manuscript Received July 16, 2010

The La_2Sb type silicides and germanides REScSi and REScGe (RE = La, Ce) were synthesized from the elements by arc-melting and subsequent annealing at 1170 K. The structures of LaScSi and LaScGe were refined on the basis of single-crystal X-ray diffraction data. The structures consist of a stacking of two-dimensional [ScSi] networks with $ScSi_{4/4}$ rectangles, which are separated by rare earth atoms, which leave $RE_{4/4}$ tetrahedral voids. The latter can be completely filled by hydrogenation leading to the quaternary hydrides REScSiH and REScGeH (RE = La, Ce). Hydrogenation is accompanied by an anisotropic unit cell expansion, i.e., a decrease in the *a* lattice parameter and a strong increase in *c*. The H-insertion into the compounds based on cerium induces for both a quasi-2D structure, a strong decrease of their antiferromagnetic ordering; for instance T_N decreases from 26 to 3.0 K in the sequence CeScSi → CeScSiH and the occurrence of the influence of the Kondo effect evidenced by electrical resistivity and specific heat measurements. The electronic structure calculation applied to CeScSi and its hydride reveals strong Ce−H bonding influencing the magnetic properties of CeScSiH.

Introduction

The tetragonal La_2Sb type structure,[1,2] space group *I*4/*mmm*, has many representatives in the field of metal-rich arsenides, antimonides, and bismuthides.[3] Besides these binary compounds, various ternary ordered compounds like REScSi (RE = rare earth element), REScGe, ThSGe, UTeGe, ThSeGe, USeSi, or ThTeSi have also been reported.[3] These compounds leave two different kinds of voids, i.e., two octahedral voids at 2*a* (0 0 0) and four tetrahedral voids at 4*d* (0 ½ ¼). Filling of the octahedral voids leads to the well-known K_2NiF_4 type structure. This aristotype is known for a large variety of compounds with several hundred representatives. In contrast, only a few ternary compounds with filled tetrahedral sites have been reported such as $SrZnBi_2$ and $BaZnSb_2$.[4,5] Nevertheless, the filled La_2Sb type should be a good candidate for layered materials which are structurally related to the many ZrCuSiAs type compounds[6] like the hydrides CeCoSiH and CeCoGeH.[7−10]

The ternary compounds based on cerium, CeScSi and CeScGe, adopt the CeScSi type structure, an ordered ternary variant of the La_2Sb type.[11,12] In this structure, Ce atoms built up layers of empty edge-sharing Ce_4 tetrahedra which are separated by the scandium−silicon or scandium−germanium networks. Similar layers of Ce_4 tetrahedral units exist also in the tetragonal CeFeSi type, space group *P*4/*nmm*.[13] Concerning the magnetic properties, CeScSi and CeScGe order antiferromagnetically at T_N = 26 and 43 K, respectively.[14−17] These Néel temperatures are relatively high for intermetallics of cerium with nonmagnetic elements.

Recently, we have shown that the equiatomic compounds based on cerium CeT(Si or Ge) (T = transition metal) such as CeCoSi, CeCoGe, and CeRuSi, which crystallize in the tetragonal CeFeSi type, absorb hydrogen when exposed under

*To whom correspondence should be addressed. E-mail: chevalie@icmcb-bordeaux.cnrs.fr.

(1) Stassen, W. N.; Sato, M.; Calvert, L. D. *Acta Crystallogr.* **1970**, *B26*, 1534.
(2) Wang, Y.; Calvert, L. D.; Taylor, J. B. *Acta Crystallogr.* **1980**, *B36*, 220.
(3) Villars, P.; Calvert, L. D. *Pearson's Handbook of Crystallographic Data for Intermetallic Phases*, 2nd ed.; American Society for Metals: Materials Park, OH, 1991 and Desk Edition, 1997.
(4) Cordier, G.; Eisenmann, B.; Schäfer, H. *Z. Anorg. Allg. Chem.* **1976**, *426*, 205.
(5) Brechtel, E.; Cordier, G.; Schäfer, H. *J. Less-Common Met.* **1981**, *79*, 131.
(6) Pöttgen, R.; Johrendt, D. *Z. Naturforsch.* **2008**, *63b*, 1135.
(7) Chevalier, B.; Gaudin, E.; Weill, F.; Bobet, J.-L. *Intermetallics* **2004**, *12*, 437.
(8) Chevalier, B.; Matar, S. F. *Phys. Rev. B* **2004**, *70*, 174408.
(9) Chevalier, B.; Pasturel, M.; Bobet, J.-L.; Isnard, O. *Solid State Commun.* **2005**, *134*, 529.
(10) Chevalier, B.; Matar, S. F.; Ménétrier, M.; Sanchez Marcos, J.; Rodriguez Fernandez, J. *J. Phys.: Condens. Matter* **2006**, *18*, 6045.
(11) Mokra, I. R.; Bodak, O. I. *Dopov. Akad. Nauk Ukr. RSR, Ser. A* **1979**, *4*, 312–315.
(12) Bodak, O. I.; Kokhan, Z. M. *Inorg. Mater.* **1983**, *19*, 987.
(13) Bodak, O. I.; Gladyshevskii, E. I.; Kripyakevich, P. I. *J. Struct. Chem.* **1970**, *11*, 283.
(14) Canfield, P. C.; Thompson, J. D.; Fisk, Z. *J. Appl. Phys.* **1991**, *70*, 5992.
(15) Uwatoko, Y.; Ishii, T.; Oomi, G.; Takahashi, H.; Mori, N.; Nimori, S.; Kido, G.; Sarrao, J. L.; Mandrus, D.; Fisk, Z.; Thompson, J. D. *Phys. B* **1997**, *237−238*, 207.
(16) Singh, S.; Dhar, S. K.; Mitra, C.; Paulose, P.; Manfrinetti, P.; Palenzona, A. *J. Phys.: Condens. Matter* **2001**, *13*, 3753.
(17) Mishra, S. N. *J. Phys.: Condens. Matter* **2009**, *21*, 115601.

Published on Web 08/04/2010

3−4 MPa of H_2 pressure at 523 K.[7−10,18−21] The resulting hydrides CeCoSiH, CeCoGeH, and CeRuSiH are stable at room temperature in air or under vacuum and adopt the tetragonal ZrCuSiAs type[6] where H atoms occupy the tetrahedral Ce_4 sites.[9,20] The hydrogenation of these Ce compounds induces two effects: an anisotropic expansion of the unit cell (*a* decreases weakly whereas *c* increases strongly, leading to an overall increase of the unit cell volume) and the occurrence of Ce−H bonding. The existence of these two effects linked to the H-insertion can lead to an intermediate valence state for the cerium, as observed for the hydrides CeCoSiH and CeCoGeH[7−10] (strong Ce−H bonding inducing a demagnetisation of Ce) or, on the contrary, to the appearance of an antiferromagnetic ordering, as reported for CeRuSiH (the "negative" pressure induced by H-insertion tends to stabilize the trivalent cerium).[19,20] In other words, the hydrogenation of these intermetallics strongly modifies their physical properties.

In this view, it is interesting to investigate the hydrogenation of the ternary compounds CeScSi and CeScGe which present structural properties in relation to those existing for the tetragonal CeFeSi type. We report here, for the first time, on the characterization of the new hydrides CeScSiH and CeScGeH by X-ray powder diffraction, electrical resistivity, magnetization, and specific heat measurements. We will show that these hydrides present a magnetic ordering temperature smaller than that of the initial compounds. We discuss this behavior on the basis of *ab initio* electronic structure calculations performed on CeScSi and its hydride. Also, for comparison, some results concerning the influence of the hydrogenation of the isotypic ternary compounds LaScSi and LaScGe are presented.

Experimental Section

Synthesis and Hydrogenation. Starting materials for the preparation of the REScSi and REScGe (RE = La, Ce) samples were ingots of lanthanum and cerium (smart-elements and Johnson-Mattey), scandium pieces (smart-elements), silicon lumps, and germanium pieces (Wacker), all with stated purities better than 99.9%. In the first step, pieces of the lanthanum and cerium ingot were arc-melted[22] under argon (~600 mbar) to small buttons. The argon was purified before with titanium sponge (870 K), silica gel, and molecular sieves. The small RE buttons were then mixed with Sc and Si or Ge pieces in the ideal 1:1:1 atomic ratio and reacted in the same arc-melting furnace. The product buttons were remelted three times to ensure homogeneity. In the above procedure, the total weight loss (less than 0.2%) was negligible.

The arc-melted samples were all not single-phase. The buttons were then ground to a fine powder in an agate mortar, cold-pressed to small pellets (diameter 6 mm) and sealed in evacuated silica tubes. The pellets were then annealed for 3 weeks at 1170 K followed by quenching. In some cases the latter procedure was repeated in order to obtain a phase pure sample. With this way, we obtained X-ray pure samples of all four ternary compounds. For crystal growth of the intermetallics based on lanthanum, the annealed buttons were slowly cooled at a rate of 2 K h^{-1} from 1170 to 820 K. All products were obtained as brittle, silvery materials which are stable in air over weeks. Small single crystals exhibit metallic luster.

Table 1. Lattice Parameters (Guinier Powder Data) of the Tetragonal Compounds REScSi, REScSiH, REScGe, and REScGeH (RE = La and Ce)

compound	*a*/pm	*c*/pm	*V*/nm^3	ref
LaScSi	434.92(5)	1602.0(3)	0.3030	[a]
LaScSi	434.4(5)	1598(2)	0.3015	11
LaScSi	433.5(2)	1599.7(1)	0.3006	16
LaScSiH	428.3(3)	1709.4(5)	0.3136	[a]
LaScGe	437.35(6)	1615.7(4)	0.3091	[a]
LaScGe	435.1(1)	1606.7(8)	0.3042	12
LaScGeH	430.7(3)	1719.8(5)	0.3190	[a]
CeScSi	432.83(5)	1582.0(2)	0.2964	[a]
CeScSi	430.0(5)	1580(2)	0.2921	11
CeScSi	431.5	1586.4	0.2953	16
CeScSiH	425.4(3)	1675.1(5)	0.3031	[a]
CeScGe	434.73(8)	1595.9(4)	0.3016	[a]
CeScGe	434.5(1)	1594.3(2)	0.3010	17
CeScGe	431.4(2)	1591.3(8)	0.2962	12
CeScGe	434.2(1)	1598.6(3)	0.3014	16
CeScGeH	428.4(3)	1703.3(5)	0.3126	[a]

[a] This work.

Hydrogen absorption experiments were performed using the apparatus formerly described.[23] An annealed ingot was heated under vacuum at 523 K for 12 h and then exposed to 4 MPa of hydrogen gas at the same temperature. The amount of absorbed H was determined volumetrically by monitoring pressure changes in a calibrated volume. Under the experimental conditions described above, all the REScSi and REScGe ternary compounds used in the study absorb hydrogen. The amount of H atoms inserted is 1.0(1) per REScSi or REScGe formula unit. The formed hydrides are stable in air.

EDX Analyses. The composition as well as the homogeneity of the LaScSi and LaScGe single crystals investigated by X-ray diffraction and the bulk samples were studied by energy dispersive analyses of X-rays (EDX) using a Leica 420i scanning electron microscope with CeO_2, LaF_3, Sc, SiO_2, and Ge as standards. The crystals (mounted on quartz fibres) were first coated with a thin carbon film to ensure conductivity. The polycrystalline bulk samples were embedded in a methylmethacrylate matrix. They were polished with diamond and SiO_2 emulsions with different grain size. The crystals and the samples present a perfect chemical homogeneity. The semiquantitative analyses were in good agreement with the ideal 1:1:1 composition. No impurity elements heavier than sodium (detection limit of the instrument) were observed.

X-ray Diffraction Measurements. The REScSi and REScGe (RE = La, Ce) samples and their hydrides were characterized through Guinier powder patterns (Cu $K\alpha_1$ radiation, α-quartz: $a = 491.30$ and $c = 540.46$ pm as internal standard). The Guinier camera was equipped with an imaging plate technique (Fujifilm, BAS-READER 1800). The experimental patterns matched a calculated one[24] indicating pure samples on the level of X-ray powder diffraction. The tetragonal lattice parameters (Table 1) were obtained through a least-squares routine.

(18) Chevalier, B.; Matar, S. F.; Sanchez Marcos, J.; Rodriguez Fernandez, J. *Phys. B* **2006**, *378−380*, 795.
(19) Chevalier, B.; Gaudin, E.; Tencé, S.; Malaman, B.; Rodriguez Fernandez, J.; André, G.; Coqblin, B. *Phys. Rev. B* **2008**, *77*, 014414.
(20) Tencé, S.; André, G.; Gaudin, E.; Chevalier, B. *J. Phys.: Condens. Matter* **2008**, *20*, 255239.
(21) Chevalier, B.; Tencé, S.; Gaudin, E.; Matar, S. F.; Bobet, J.-L. *J. Alloys Compd.* **2009**, *480*, 43.
(22) Pöttgen, R.; Gulden, Th.; Simon, A. *GIT Labor-Fachzeitschrift* **1999**, *43*, 133.
(23) Bobet, J.-L.; Pechev, S.; Chevalier, B.; Darriet, B. *J. Alloys Compd.* **1998**, *267*, 136.
(24) Yvon, K.; Jeitschko, W.; Parthé, E. *J. Appl. Crystallogr.* **1977**, *10*, 73.

Table 2. Crystal Data and Structure Refinement for LaScSi and LaScGe with Ordered La_2Sb Type Structure; Space Group $I4/mmm$; $Z = 4$

compound	LaScSi	LaScGe
molar mass, g mol^{-1}	211.96	256.46
calculated density, g cm^{-3}	4.65	5.51
absorption coefficient, mm^{-1}	16.2	25.0
detector distance, mm	60	80
exposure time, min	10	20
ω range; increment, deg	0−180, 1.0	0−180, 1.0
integration parameters A; B; EMS	13.0; 3.0; 0.012	13.0; 3.0; 0.014
$F(000)$, e	368	440
crystal size, μm^3	20 × 20 × 30	10 × 10 × 10
transmission ratio (max/min)	1.28	1.44
θ range, deg	2−35	2−31
range in hkl	±6, ± 6, ± 25	±6, ± 6, ± 23
total no. reflections	2117	1500
independent reflections/R_{int}	231/0.057	182/0.077
reflections with $I \geq 2\sigma(I)/R_\sigma$	209/0.027	150/0.043
data/parameters	231/11	182/11
goodness-of-fit on F^2	1.22	1.11
$R1$/wR2 for $I \geq 2\sigma(I)$	0.037/0.077	0.027/0.036
$R1$/wR2 for all data	0.046/0.079	0.042/0.038
extinction coefficient	0.0042(14)	0.0005(5)
largest diff. peak/hole, e Å^{-3}	2.38/−2.01	1.97/−2.40

Small irregularly shaped single crystals of LaScSi and LaScGe were isolated from the crushed annealed samples and investigated on a Buerger precession camera (white Mo radiation, Fujifilm imaging plate) in order to check the quality for intensity data collection. The data sets were collected at room temperature by use of an IPDS II diffractometer (graphite monochromatized Mo Kα radiation; oscillation mode). Numerical absorption corrections were applied to the data sets. Details on the crystallographic data measurements are given in Table 2.

Unfortunately, the poor quality of the single crystals isolated from a hydride CeScSiH sample did not allow their use for crystal structure determination. Its crystal structure was determined by means of X-ray powder diffraction. The data were collected with a Philips X-Pert diffractometer operating at room temperature and using Cu Kα_1 radiation (λ = 154.051 pm). The powder diffraction pattern was scanned over the angular range 8.016−129.992° with a step size of $\Delta(2\theta)$ = 0.008°. Rietveld refinement was performed using the Jana2006 program package.[25] The background was estimated by a Legendre function, and the peak shapes were described by a pseudo-Voigt function. The initial atomic coordinates were taken from a previous study of the pristine compound CeScGe.[16] A significant broadening of the peaks along the (001) direction was observed. A modification of the function shape for these peaks was introduced using the axial method of the anisotropic strain broadening option implemented in Jana2006.[25] A correction for roughness (Bragg−Brentano geometry) was introduced to avoid negative values for the ADPs induced by the high absorption coefficient of the sample.

Structural Refinement. Analyses of the diffractometer data sets of LaScSi and LaScGe showed body-centered tetragonal lattices and no additional systematic extinctions. This was in agreement with space group $I4/mmm$, similar to previous work on CeScSi.[16] The positional parameters of CeScSi[16] were then taken as starting values and both structures were refined using SHELXL-97 (full-matrix least-squares on F^2)[26] with anisotropic atomic displacement parameters for all atoms. Refinement of the occupancy parameters showed full occupancy within 1 standard deviation. The final difference electron-density syntheses were flat. The results of the structure refinements are summarized in Table 2. The atomic coordinates and the interatomic distances are listed in Tables 3 and 4. Further information on the structure refinements is available from Fachinformationszentrum Karlsruhe, D-76344 Eggenstein-Leopoldshafen (Germany), by quoting the Registry No's. CSD-421730 (LaScSi) and CSD-421729 (LaScGe).

Table 3. Atomic Coordinates and Isotropic Displacement Parameters (pm^2) of LaScSi and LaScGe[a]

atom	site	occupancy (%)	x	y	z	U_{eq}
LaScSi						
La	4*e*	100(5)	0	0	0.323 72(5)	92(3)
Sc	4*c*	101(8)	0	1/2	0	113(5)
Si	4*e*	100(5)	0	0	0.118 7(2)	101(7)
LaScGe						
La	4*e*	98(9)	0	0	0.323 88(4)	81(2)
Sc	4*c*	99(10)	0	1/2	0	105(4)
Ge	4*e*	102(10)	0	0	0.119 62(6)	92(3)

[a] U_{eq} is defined as one third of the trace of the orthogonalized U_{ij} tensor.

Table 4. Interatomic Distances (pm), Calculated with the Powder Lattice Parameters of LaScSi and LaScGe[a]

	LaScSi				LaScGe		
La:	4	Si	321.1	La:	4	Ge	322.4
	1	Si	328.4		1	Ge	330.0
	4	Sc	356.4		4	Sc	358.9
	4	La	387.8		4	La	390.7
Sc:	4	Si	288.9	Sc:	4	Ge	291.8
	4	Sc	307.5		4	Sc	309.3
	4	La	356.4		4	La	358.9
Si:	4	Sc	288.9	Ge:	4	Sc	291.8
	4	La	321.1		4	La	322.4
	1	La	328.4		1	La	330.0

[a] All distances within the first coordination spheres are listed. Standard deviations are all equal or less than 0.2 pm.

Analysis of the X-ray powder pattern of CeScSiH recorded at room temperature (Figure 1) shows that this hydride adopts, similar to the parent ternary silicide CeScSi the space group $I4/mmm$. The impurity phase $Ce_2Sc_3Si_4$ was taken into account for the refinement[27] with a determined amount equal to 2.5 wt % (this last ternary silicide which exhibits an antiferromagnetic ordering at 5.6 K[28] was not detected by magnetization and specific heat measurements as reported below). The refined unit cell parameters of a = 425.443(12) and c = 1675.15(6) pm of CeScSiH are in agreement with those determined earlier using Guinier powder data (Table 1). The final refinement of the atomic positions with isotropic atomic displacement parameters (ADPs) led to the profile factors R_p/R_{wp} = 5.12/7.16% and the reliability factors $R_{F(obs)}/R_{B(obs)}$ = 4.66/7.74% . The final atomic positions and isotropic ADPs are gathered in Table 5 and the interatomic distances in Table 6.

Physical Property Measurements. For electrical resistivity measurements, the hydride samples were compacted at room temperature (compactness ≈ 80%) in order to form a polycrystalline pellet (diameter = 6 mm and thickness = 3 mm) and then heated for 2 days at 523 K under a pressure (4 MPa) of hydrogen. After this thermal treatment, which improves the mechanical behavior, the pellet was checked by X-ray diffraction; no structural change was evidenced. For electrical resistivity (ρ), a bar of 1.5 × 1.5 × 5 mm^3

(25) Petricek, V.; Dusek, M.; Palatinus, L. *The Crystallographic Computing System*; Institute of Physics: Praha, Czech Republic, 2006.
(26) Sheldrick, G. M. *SHELXL-97, Program for Crystal Structure Refinement*; University of Göttingen: Göttingen, Germany, 1997.
(27) Mokra, I. R.; Bodak, O. I.; Gladyshevskii, E. I. *Sov. Phys. Crystallogr.* **1979**, *24*, 729.
(28) Dhar, S. K.; Manfrinetti, P.; Palenzona, A.; Kimura, Y.; Kozaki, M.; Onuki, Y.; Takeuchi, T. *Phys. B* **1999**, *271*, 150.

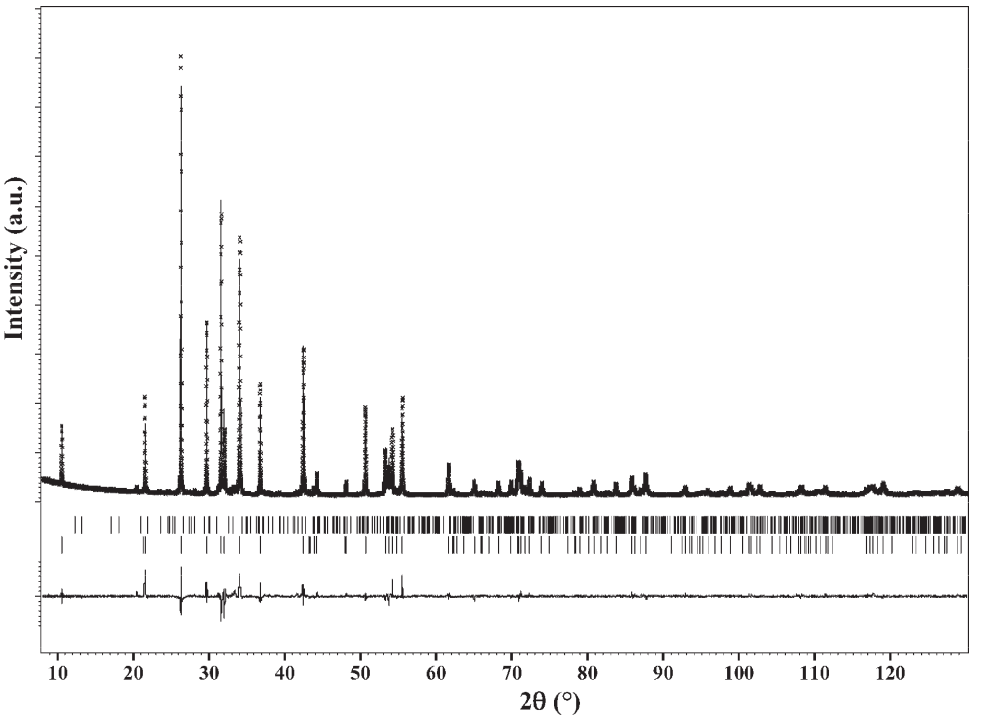

Figure 1. Rietveld refinement of the CeScSiH XRD powder pattern measured with Cu $K_{\alpha 1}$ radiation (λ = 154.051 pm) at T = 293 K. The bottom vertical bars correspond to the Bragg peak positions for the hydride by considering the space group *I*4/*mmm* and the cell parameters given in Table 5. The upper vertical bars correspond to the impurity phase $Ce_2Sc_3Si_4$.

Table 5. Atomic Coordinates and Isotropic Displacement Parameters (pm^2) for the Metal Atoms in CeScSiH (Space Group *I*4/*mmm*, *a* = 425.443(12), and *c* = 1675.15(6) pm)

atom	site	*x*	*y*	*z*	U_{iso}
Ce	4*e*	0	0	0.3200(2)	54(11)
Sc	4*c*	0	1/2	0	110(20)
Si	4*e*	0	0	0.1124(6)	30(30)

Table 6. Interatomic Distances (pm) in the Structures of CeScSi[16] and CeScSiH[a]

	CeScSi				CeScSiH		
Ce:	4	Si	317.9	Ce:	4	Si	321.4
	1	Si	321.4		1	Si	347.8
	4	Sc	353.2		4	Sc	369.0
	4	Ce	385.0		4	Ce	381.4
	4	Ce	432.3		4	Ce	425.4
Sc:	4	Si	289.0	Sc:	4	Si	284.1
	4	Sc	305.7		4	Sc	300.8
	4	Ce	353.2		4	Ce	369.0
Si:	4	Sc	289.0	Si:	4	Sc	284.1
	4	Ce	317.9		4	Ce	321.4
	1	Ce	321.4		1	Ce	347.8

[a] Standard deviations are all equal or less than 0.3 pm.

was cut from the pellet. The measurement was carried out above 4.2 K using the standard dc four probe method with silver paint contacts and an intensity current of 10 mA. Because of the small compactness and the presence of microcracks into these bars, the absolute value of ρ could not be determined accurately; for this reason, a normalized representation $\rho(T)/\rho(270\ K)$ was given. Similar transport measurements were performed on the hydrides LaScSiH and LaScGeH. Finally, magnetization measurements were performed on a part of the pellet using a superconducting quantum interference device magnetometer in the temperature range of 1.8−300 K and applied fields up to 4.6 T.

Heat capacity measurements on the hydrides CeScSiH and CeScGeH were performed by a relaxation method with a Quantum Design PPMS system and using a two tau model analysis. Data were taken in the 1.8−50 K temperature range, compatible with the magnetic ordering temperature of the parent compounds CeScSi and CeScGe.[14−17] For the latter measurements, the sample was a plate (40−50 mg weight) obtained from the same pellet used for the electrical resistivity and magnetization measurements.

Computational Details. Two computational methods were used in the framework of density functional theory (DFT).[29,30] A pseudo potential approach within the Vienna *ab initio* simulation package (VASP) code[31] was first called for to obtain the equation of states (EOS) for CeScSi and its hydride with projector augmented wave (PAW) potentials,[32,33] necessary for an account of 4f(Ce) states, built within the generalized gradient approximation (GGA) scheme.[34] The calculations were converged at an energy cutoff of 300 eV for the plane-wave basis set with respect to the k-point integration with a starting mesh of 4 × 4 × 4 up to 8 × 8 × 8 for best convergence and relaxation to zero strains. The Brillouin-zone integrals were approximated using a special k-point sampling.

The all-electron calculations are based on the DFT and GGA functional.[34] They were performed using the full potential scalar-relativistic augmented spherical wave (ASW) method (see refs 35 and 36. and references therein). In the ASW method,

(29) Hohenberg, P.; Kohn, W. *Phys. Rev.* **1964**, *136*, B864.
(30) Kohn, W.; Sham, L. J. *Phys. Rev.* **1965**, *140*, A1133.
(31) Kresse, G.; Furthmüller, J. *Phys. Rev. B* **1996**, *54*, 11169.
(32) Blöchl, P. E. *Phys. Rev. B* **1994**, *50*, 17953.
(33) Kresse, G.; Joubert, J. *Phys. Rev.* **1999**, *B59*, 1758.
(34) Perdew, J. P.; Burke, K.; Ernzerhof, M. *Phys. Rev. Lett.* **1996**, *77*, 3865.
(35) Williams, A. R.; Kübler, J.; Gelatt, C. D. *Phys. Rev. B* **1979**, *19*, 6094.
(36) Eyert, V. The Augmented Spherical Wave Method-A Comprehensive Treatment. In *Lecture Notes in Physics*; Springer: Berlin Heidelberg, Germany, 2007; Vol. *719*.

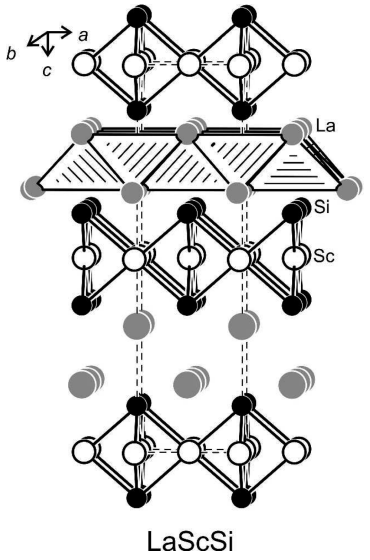

Figure 2. The crystal structure of LaScSi. Lanthanum, scandium, and silicon atoms are drawn as light gray, black open, and filled circles, respectively. The two-dimensional [ScSi] network and the layers of condensed $La_{4/4}$ tetrahedra are emphasized.

the wave function is expanded in atom-centered augmented spherical waves, which are Hankel functions and numerical solutions of Schrödinger's equation, respectively, outside and inside the so-called augmentation spheres. In the minimal ASW basis set, we chose the outermost shells to represent the valence states and the matrix elements were constructed using partial waves up to $l_{max} + 1 = 4$ for Ce, i.e., 4f(Ce) were considered within the basis set, $l_{max} + 1 = 3$ for Sc and Si and finally $l_{max} + 1 = 2$ for H. Self-consistency was achieved by a highly efficient algorithm for convergence acceleration.[37] The Brillouin zone integrations were performed using the linear tetrahedron method with up to 1088 k-points within the irreducible wedge.[32,36] The efficiency of this method in treating magnetism and chemical bonding properties in transition metal, lanthanide, and actinide compounds has been well demonstrated in recent years.[8,38,39]

The relative magnitude of the chemical bonding is obtained based on the overlap population analysis: S_{ij}, i and j being two chemical species. The crystal orbital overlap population (COOP) criterion is used.[40] For the purpose of establishing trends of chemical bonding strength, we show the integrated COOP (*i*COOP): the larger the area below the curves the larger is the bonding. In the plots, positive, negative, and zero *i*COOP magnitudes indicate bonding, antibonding, and nonbonding interactions, respectively.

Results and Discussion

Crystal Chemistry. The isotypic silicides and germanides REScSi and REScGe (RE = La, Ce) crystallize with a ternary ordered version of the La_2Sb type[1,2] structure, space group $I4/mmm$. The lanthanum (cerium) and scandium atoms are ordered on the two crystallographically independent lanthanum sites 4*e* and 4*c*, and the silicon (germanium) atoms occupy the 4*e* antimony site. As an example, we present the LaScSi structure in Figure 2. The scandium and silicon atoms built up a two-dimensional [ScSi] network in which every scandium atom has a rectangular silicon coordination at Sc−Si distances of 289 pm (Table 4). These are longer than the sum of the covalent radii[41] of 255 pm, indicating only weak Sc−Si bonding. The shortest distances within the [ScSi] network occur between the scandium atoms, which form a square network with Sc−Sc distances of 308 pm (Table 4), significantly smaller than in hcp scandium (6 pm × 325 pm and 6 pm × 331 pm).[42] We can thus assume substantial Sc−Sc bonding.

The [ScSi] layers are separated by two layers of lanthanum atoms. As emphasized in the upper part of Figure 2, the double layers of lanthanum atoms are layers of condensed La_4 tetrahedra. The latter can, as observed during the hydrogenation of the compounds showing the tetragonal CeFeSi-type,[21] completely be filled with hydrogen leading to new quaternary hydrides REScSiH and REScGeH (RE = La, Ce). Hydrogenation has a drastic, anisotropic effect on the course of the lattice parameters. The *a* parameter becomes smaller while *c* increases (Table 1). This structural principle is closely related to the many ZrCuSiAs type materials.[6] In other words, the H-insertion into for instance CeScSi involves an expansion of the unit cell volume from 0.2964 to 0.3031 nm^3 (2.3%) (Table 1). Also, the strong increase of the c/a ratio (3.66 → 3.94) observed after hydrogenation of CeScSi could play an important role on the modification of its physical properties. We note that similar structural changes are evidenced after the H-insertion into LaScSi, LaScGe, and CeScGe (Table 1).

It is also worth pointing out that the H-insertion into CeScSi also strongly affects the atomic position of the Si atom: z_{Si} varies from 0.124[11] to 0.1124(6) (Table 5); the Si atom shifts along the *c* axis in the [ScSi] layer inducing a decrease of the Sc−Si distance from 289 to 284 pm (Table 6). On the contrary, z_{Ce} is less affected (0.326 → 0.3200(2)) by the hydrogenation. Similar behaviors were observed during the hydrogenation of the ternary compounds adopting the CeFeSi type.[9,19] The strong increase of the *c* parameter in the sequence CeScSi → CeScSiH suggests that the H atoms are inserted in the Ce_4 tetrahedra, as observed previously for the deuteride CeCoGeD.[9] This H-insertion explains the displacement of the Si atom along the *c* axis; indeed, the Si−H bonding exists only in this direction. According to this hypothesis, the H atom occupies the 4*d* site (0 ½ ¼), giving interatomic distances Ce−H = 243 pm comparable to those reported for CeRuSiH.[19] Neutron powder diffraction experiments are necessary on the deuteride CeScSiD in order to confirm the hydrogen position into this compound.

Electric Properties. Figure 3 depicts the temperature dependent normalized electrical resistivity $\rho(T)/\rho(270\ K)$, measured above 4.2 K, for the hydrides LaScSiH, CeScSiH, and CeScGeH. Between 270 and 40 K, $\rho(T)$ for LaScSiH decreases weakly and then exhibits a small increase. This behavior, evidenced also for the other hydride LaScGeH, characterizes a nonmetallic hydride (see the part devoted to

(37) Eyert, V. *J. Comput. Phys.* **1996**, *124*, 271.
(38) Eyert, V.; Laschinger, C.; Kopp, T.; Frésard, R. *Chem. Phys. Lett.* **2004**, *385*, 249.
(39) Matar, S. F.; Gaudin, E.; Chevalier, B.; Pöttgen, R. *Solid State Sci.* **2007**, *9*, 274.
(40) Hoffmann, R. *Angew. Chem., Int. Ed. Engl.* **1987**, *26*, 846.
(41) Emsley, J. *The Elements*; Clarendon Press: Oxford, U.K., 1989.
(42) Donohue, J. *The Structures of the Elements*; Wiley: New York, 1974.

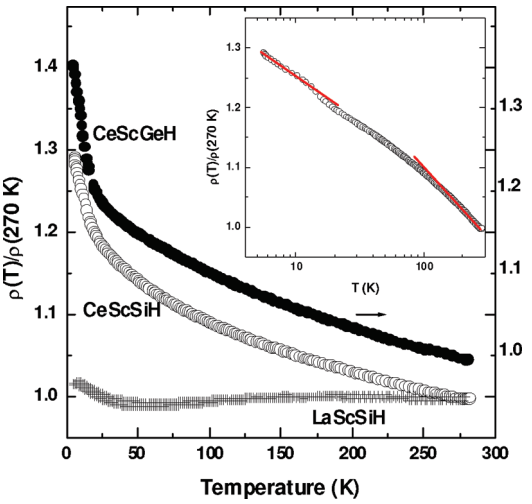

Figure 3. Temperature dependence of the normalized electrical resistivity $\rho(T)/\rho(270\ K)$ for the hydrides LaScSiH, CeScSiH, and CeScGeH (right-hand axis). The inset shows the dependence of $\rho(T)/\rho(270\ K)$ as a function of log T for CeScSiH; the solid red lines represent the fit $-A$ log T.

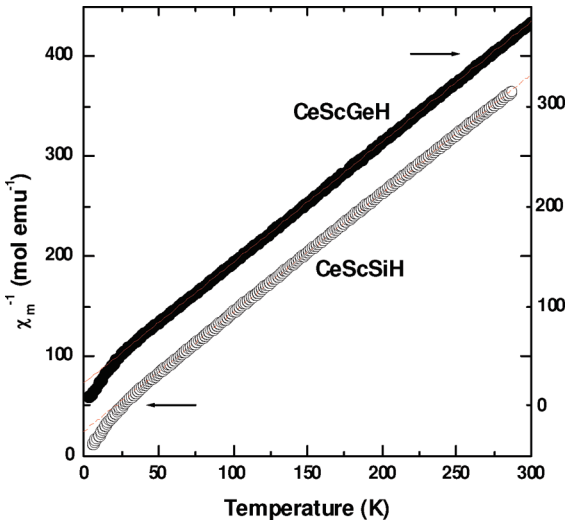

Figure 4. Temperature dependence of the reciprocal magnetic susceptibility χ_m^{-1}, measured with an applied field of 4 T, of hydrides CeScSiH and CeScGeH. Dashed lines show the fit to χ_m^{-1} calculated with the Curie−Weiss law. For clarity, the curve relative to CeScGeH is shifted vertically.

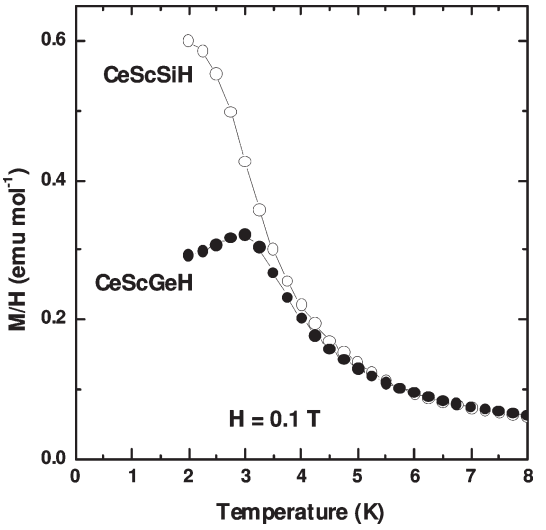

Figure 5. Temperature dependence of the magnetization M divided by applied field $H = 0.1$ T for the hydrides CeScSiH and CeScGeH.

the Electronic Structure Calculations) as observed for $La_2Ni_2MgH_8$.[43] However, because of the inability to compact the powder sample sufficiently; a reliable value for the band gap could not be obtained.

Before explaining the behavior of the electrical resistivity of CeScSiH and CeScGeH and in order to understand it, we should make reference to the electrical resistivity measurements of the initial ternary compounds CeScSi and CeScGe, which can be summarized as follows: (i) the curves $\rho(T)$ show a linear decrease of ρ with decreasing temperature until 26 and 46 K, respectively, where (ii) a sudden decrease of ρ appears in agreement with the occurrence of the antiferromagnetic ordering.[14,15] The electrical resistivity of the hydrides exhibits a different behavior versus the temperature; for these compounds the curves $\rho(T)/\rho(270\ K)$ increase with decreasing temperature until 4.2 K. For CeScSiH, for instance, in the two temperature ranges 110−270 K and 4.2−14 K (inset of Figure 3), the law $\rho(T)/\rho(270\ K) = -A$ log T (A = constant) is observed. Such behavior, not observed for $Ce_2Sc_3Si_4$,[28] which is the impurity detected in the CeScSiH sample, is expected for Kondo-type interactions in the presence of crystal field effects.[44] The high-temperature logarithmic region represents the Kondo effect in the excited doublet, whereas the low-temperature region is relative to the Kondo effect from the crystal field ground state. We note that the hydrogenation of CeScSi and CeScGe induces a Kondo behavior for the respective hydrides.

Magnetic and Thermal Properties. The magnetization measurements performed on the initial ternary compounds CeScSi and CeScGe reveal results comparable to those reported by Singh et al.[16] and reflect the purity of our samples.

Above 50 K, the reciprocal magnetic susceptibility χ_m^{-1} of CeScSiH and CeScGeH can be fitted with a Curie−Weiss law as presented in Figure 4. The experimental values of the effective magnetic moments μ_{eff} are 2.59 and 2.58 μ_B/Ce, respectively, for CeScSiH and CeScGeH in agreement with that calculated one for a free Ce^{3+} ion (2.54 μ_B/Ce). The paramagnetic Curie temperature θ_p is found to be −21 K for CeScSiH and −19.5 K for CeScGeH. These values are negative contrary to that reported for CeScSi ($\theta_p = 15.7$ K),[16] but such behavior is often found in Kondo compounds. Finally below 50 K, the $\chi_m^{-1} = f(T)$ curves deviate from a straight-line behavior, presumably due to thermal depopulation of the crystal-field levels.

The curves presenting below 8 K (Figure 5), the temperature dependence of the magnetization of CeScSiH and CeScGeH reveals no anomaly around 5.6 or 5.0 K attributable to the antiferromagnetic ordering of $Ce_2Sc_3Si_4$ or $Ce_2Sc_3Ge_4$, respectively.[28,45] In other words, the small amount of $Ce_2Sc_3Si_4$ detected by X-ray powder

(43) Chotard, J.-N.; Filinchuk, Y.; Revaz, B.; Yvon, K. *Angew. Chem.* **2006**, *118*, 7934.
(44) Cornut, B.; Coqblin, B. *Phys. Rev.* **1972**, *B5*, 4541.
(45) Yokoyama, M.; Kosaka, M.; Mori, N.; Uwatoko, Y.; Abe, H.; Kitazawa, H.; Kido, G. *J. Phys. Soc. Jpn.* **2003**, *72*, 947.

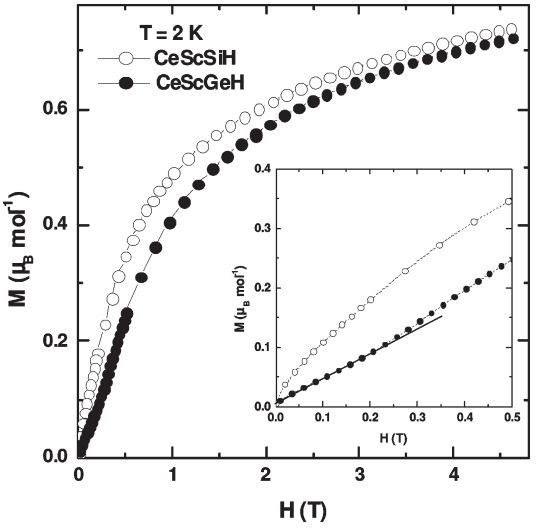

Figure 6. Field dependence at 2 K of the magnetization M of CeScSiH and CeScGeH. The inset presents the dependences at low field.

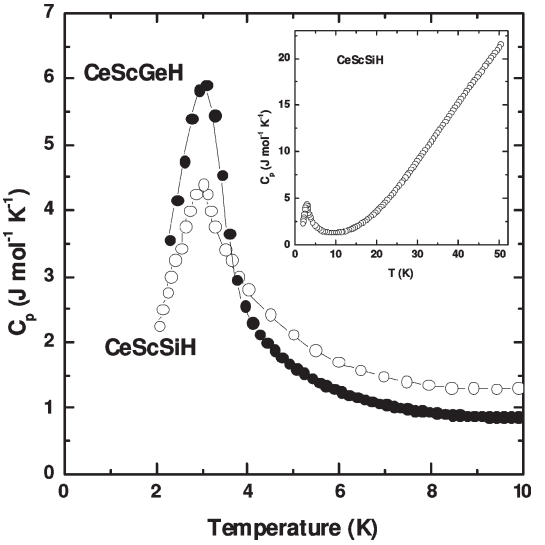

Figure 7. Temperature dependence below 10 K of the specific heat C_p in the hydrides CeScSiH and CeScGeH. The inset presents for $T < 50$ K, the curve C_p versus T for CeScSiH.

diffraction on the hydride CeScSiH (Figure 1) does not affect its magnetic properties.

Below 8 K, the curves M versus T of the hydrides exhibits different behaviors (Figure 5): (i) M of CeScSiH tends to saturate below $T_t = 3.0(2)$ K (the temperature where the derivative curve $d(M/H)/dT = f(T)$ exhibits a maximum) and (ii) the presence of a broad maximum at $T_N = 3.0(2)$ K in the temperature dependence of M for CeScGeH suggests an antiferromagnetic ordering of the Ce magnetic moments. This magnetic ordering is further corroborated by the field dependent behavior of M taken at 2 K (Figure 6). In the antiferromagnetic range, M of CeScGeH increases linearly at low fields, more rapidly in the range of the critical field $H_{cr} = 0.18-0.2$ T (inset of Figure 6), and then exhibits a curvature. This behavior suggests the occurrence of a magnetic transition induced by the applied magnetic field as observed in many antiferromagnets (spin-flip or spin-flop transition). A similar transition is difficult to detect for the hydride CeScSiH certainly because of a very small critical field H_{cr} of its metamagnetic transition. Therefore, it is clear that no maximum in the derivative curve $dM/dH = f(H)$ is detectable, due to the applied field strength of 0.017 T which is higher than H_{cr}.

As presented in Figure 7, the temperature dependence of the specific heat C_p for CeScSiH and CeScGeH exhibits a peak at 3.0(2) and 3.1(2) K, respectively (note the absence of an anomaly around 26 or 5.6 K on the curve C_p versus T given in the inset of the Figure 7 for CeScSiH means that the pristine compound CeScSi or $Ce_2Sc_3Si_4$ is not detected by this measurement). The temperatures of the heat capacity peaks agree with those where the curves $M = f(T)$ (Figure 5) detect a magnetic transition. Valuable information can be obtained from the entropy associated with the antiferromagnetic ordering of CeScSiH and CeScGeH, which is estimated from the magnetic contribution to C_p in the low temperature range ($10 \text{ K} < T < 25$ K) as $C_{p\ mag} = C_p - (\gamma T + \beta T^3)$. The electronic coefficient γ and the phonon constant β were estimated by fitting of the C_p/T versus T^2 plot for $10 < T < 25$ K. For CeScSiH for instance, this procedure gives $\gamma = 69$ mJ K^{-2} mol^{-1} and $\beta = 0.277$ mJ K^{-4} mol^{-1}. At the magnetic transition, $C_{p\ mag}$ reaches 2.65 and 3.43 J K^{-1} mol^{-1} for CeScSiH and CeScGeH, respectively. These $C_{p\ mag}$ values are smaller than the one expected for a doublet ground state of Ce^{3+} ($R \ln 2 = 5.76$ J K^{-1} mol^{-1}). This reduction of $C_{p\ mag}$ suggests the presence of a Kondo effect in the hydrides as previously evidenced by electrical resistivity measurements. This agrees for instance with the significant value of $\gamma = 69$ mJ K^{-2} mol^{-1} for CeScSiH higher than that reported for CeScSi (14.5 mJ K^{-2} mol^{-1}).[16]

Electronic Structure Calculations. With the use of the crystallographically determined data, a geometry relaxation was started for CeScSi and its hydride. The results show little deviation with respect to the experimental coordinates of Ce and Si. For instance, for CeScSiH: $z_{Ce} = 0.319$ instead of 0.3200 and $z_{Si} = 0.116$ instead of 0.1124 (Table 5). The volume magnitudes are systematically lower than in the experiment: 0.282 versus 0.296 nm^3 for CeScSi and 0.286 versus 0.303 nm^3 for CeScSiH (Table 1). This is expected due to the use of electron gas based DFT functionals such as GGA and LDA.

From the energy results, we examine the stability of hydrogen within CeScSi using the following expression per formula unit:

$$E_{bind} = E_{(CeScSiH)} - E_{(CeScSi)} - (1/2)E_{(H_2)}$$

While the two first terms of the right-hand side equality are the energy values obtained from the calculations, $E(H_2)$ derived from PP-PAW-GGA calculations, amounts to -6.59 eV. The resulting stabilization energy of hydrogen in CeScSiH (per 2 f.u.) is $E_{bind} = -46.76 - (-38.29) - (-6.59) = -1.88$ eV for 2 H, i.e., -0.94 eV per H. Thus H is well stabilized in CeScSi. This is also confirmed from a Bader charge analysis.[46] As a reference, the Bader analysis of

(46) Sanville, E.; Kenny, S. D.; Smith, R.; Henkelman, G. *J. Comput. Chem.* **2007**, *28*, 899.

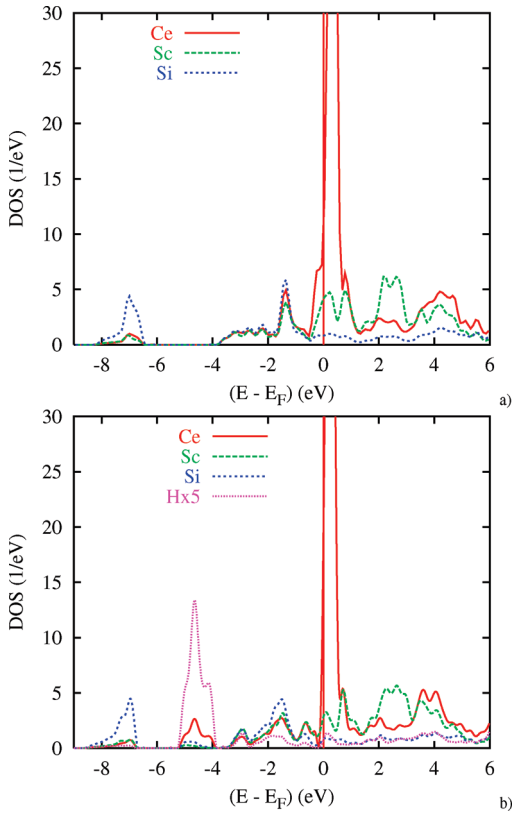

Figure 8. Site projected density of states (PDOS) for CeScSi (a) and CeScSiH (b).

archetype metal hydride, MgH_2, calculated with the same method, gives Mg^{2+} and H^-, i.e., an anionic hydrogen whose charge "increases" to $H^{-0.8}$ when Ni is introduced.[47] In presently studied hydrogenated intermetallic, hydrogen shows a negative charge of $H^{-0.39}$. This puts it half way between atomic H (1 electron) and anionic H^- (2 electrons). The extra charge arises from the metal substructures, mainly from Ce and indicates a preferential Ce−H bond (see below). Then the hydrogenated CeScSi intermetallic involves a covalent hydride.

In a second step, we have computed the electronic structures as well as the properties of chemical bonding. At self-consistent convergence, little charge transfer is observed between the elements, i.e., with amounts close to ~0.1 electrons. In CeScSiH transfer is of larger magnitude from Ce and Sc toward Si and H. However, all amounts of transfer are not meaningful of an ionic character such as H^- as one would expect from an ionic hydride chemical picture, not encountered in such calculations. Further this indicates a covalently bonded hydride system. It will be shown that in such a chemical system, the physical properties are obtained from a contribution of all present species due to the quantum mixing of valence states.

The site projected density of states (PDOS) is shown in Figure 8. In these plots and in the following ones, the energy reference along the x axis is with respect to the Fermi level E_F, in as far as both compounds are computed to be metallic. The multiplicities of all atomic constituents

(47) Matar, S. F. Prog. Solid State Chem. In press.

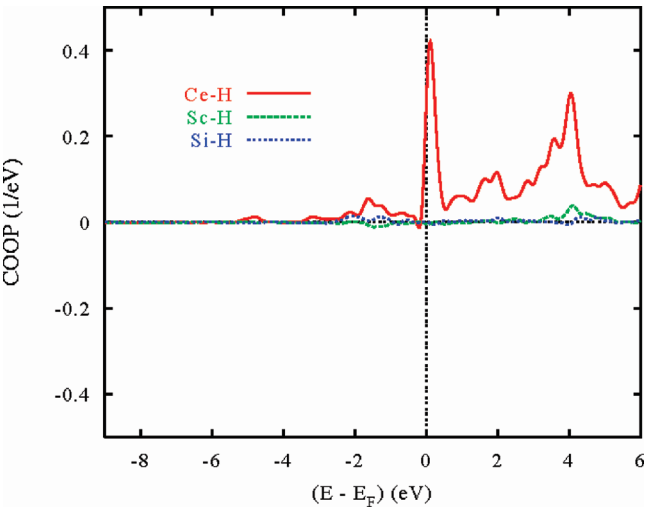

Figure 9. Chemical bonding with COOP criterion for metal substructure interactions with H in CeScSiH.

are accounted for in the plots. However, the corresponding PDOS were artificially multiplied by 5 for stressing the H valence states. In CeScSi, the valence band (VB) is dominated by Si s-like states in the [−8, −6 eV] range and the p, d PDOS from Sc, Si, and Ce from −4 eV up to the VB top with very similar skylines implying their mixing in this energy window. At E_F, there are Sc (d) as well as Ce (4f) PDOS. The largest part of Ce (4f) is, as expected from the low filling, above E_F. When H is introduced new states are found in the [−5.5, −4 eV] energy range, i.e., where no states are present in CeScSi. The largest intensity below the H PDOS is the Ce PDOS, followed by the Si PDOS. Then one may expect the largest bonding for Ce−H. The crossing of E_F at a low Ce PDOS does not suggest a magnetic instability.

The large density of states at the Fermi level, due to Ce (4f) states indicates an instability of both compounds in a spin degenerate state.[48] Then spin polarized calculations allowing for two spin occupations for all species were subsequently carried out. At self-consistent convergence magnetic moments are indeed found to develop on the different constituents: CeScSi: M(Ce) = 0.695 μ_B; M(Sc) = 0.14 μ_B; M(Si) = 0.008 μ_B. CeScSiH: M(Ce) = 0.635 μ_B; M(Sc) = 0.15 μ_B; M(Si) = 0.003 μ_B; M(H) = 0.008 μ_B. The highest moment magnitude is, as expected, for Ce with, however, a lower magnitude in the hydride. This result is concomitant with the Bader analysis reported above whereby Ce−H bonding leads to less electrons of Ce contributing to the development of the spin moment. Further this agrees with a lowering of magnetic interactions in the hydride leading to a decrease of the magnetic ordering temperature. The other species carry low magnitude moments whose origins are due to the quantum mixing with Ce states as it is shown below in the chemical bonding section.

The PDOS results can be further assessed in a chemical bonding qualitative analysis. We first examine the change

(48) Kübler, J.; Eyert, V. *Electronic Structure Calculations in Materials Science and Technology*, Vol. *3A*: Electronic and Magnetic Properties of Metals and Ceramics, Part I; Buschow, K. H. J., Ed.; VCH, Verlag: Weinheim, Germany, 1992; p 1.

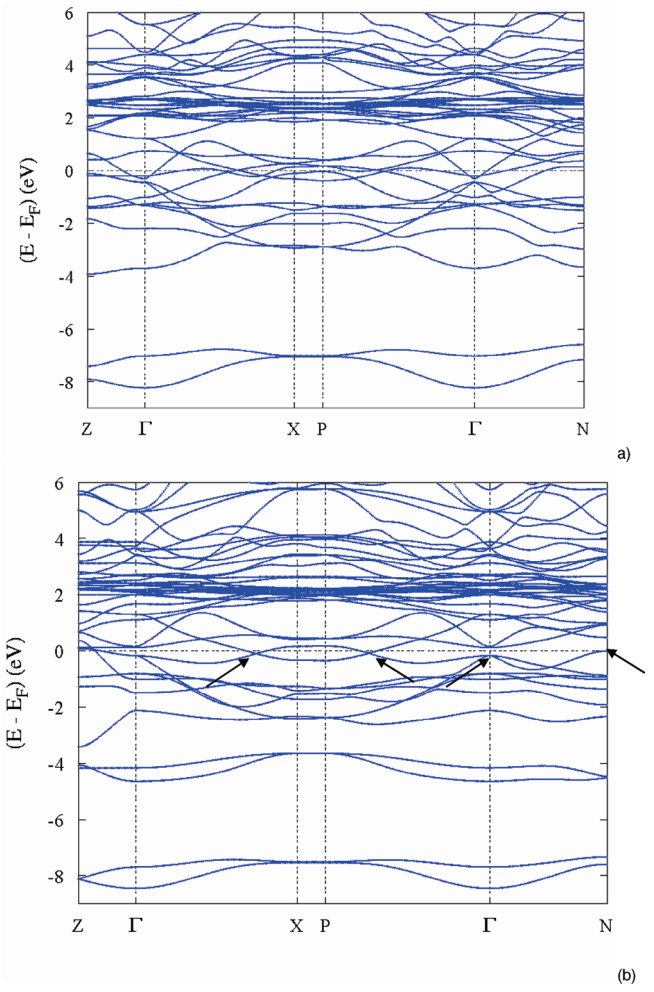

Figure 10. Band structure along major lines of Brillouin zone of tetragonal Bravais lattice for (a) LaScSi and (b) LaScSiH.

of the bonding characteristics between Ce, Sc, and Si upon going from CeScSi to its hydride, then we explicit the Ce, Sc, Si bonding with H. We find the following trends of bonding strengths, b(A−B): b(Ce−Si) > b(Sc−Si) > b(Ce−Sc) in CeScSi on one hand and b(Sc−Si) > b(Ce−Si) > b(Ce−Sc) in CeScSiH, on the other hand. This follows from the distance trends, i.e., the shorter the distance, the stronger the bond. With the interaction of the metal substructure with H in the hydrogenated intermetallic, Figure 9 shows the three kinds of bonding. The most intense interactions are for Ce−H. This follows from distance trends whereby the weakest bonding is found for of the longest Sc−H bond. Then Ce−H is the shortest with 243 pm. This further explains the lowering of the magnetic moment on Ce as shown above and may be expected from the PDOS plots where the bonding extends over a larger energy window starting at ∼−5.5 eV (Figure 8). As a consequence, the insertion of hydrogen within CeScSi is found to modify the bonding not only between the constituents and H but as well between Ce, Sc, and Si.

Regarding the peculiar behavior of LaScSiH, preliminary band structure calculations indicate that the density of states at the Fermi level (nE_F) of LaScSi shows the presence of both La and Sc *n*d states while the hydride shows a lowered (nE_F) magnitude and a band crossing at E_F. To illustrate the results, the band structures of both LaScSi and its hydride are shown in Figure 10. Contrary to panel a of the ternary silicide, in panel b the arrows signal peculiar features of band gaps at Γ (center of the Brillouin zone) and *N* on one hand and band crossings at *X* and *P* end points on the other hand. These features stress the lowering of the density of states at E_F. While we do not expect significant band gap opening within the used XC functional, i.e., stronger correlation with GGA + U would be needed, it can be suggested that significant changes of metallic LaScSi toward a weakly conducting hydrogenated intermetallic occur. This meets with the experimental results on the electric properties (Figure 3).

Conclusions

In the present paper, we showed, for the first time, that the CeScSi type compounds easily absorb hydrogen, leading to the quaternary hydrides LaScSiH, CeScSiH, LaScGeH, and CeScGeH with layers of condensed $HLa_{4/4}$ and $HCe_{4/4}$ tetrahedra with substantial La−H and Ce−H bonding as explained by chemical bonding analysis. Hydrogenation has a huge influence on the physical properties of the cerium based compounds. This leads to a strong decrease of the magnetic ordering temperature and the occurrence of Kondo type behavior evidenced by electrical resistivity and specific heat measurements. These quaternary hydrides are a promising family of compounds with pronounced two-dimensional character, very close to the ZrCuSiAs family of compounds[6] among which we find the new iron oxide−arsenide superconductors.

Acknowledgment. The authors would like to thank R. Decourt for his assistance during the specific heat measurements. Computations were carried out on the mainframe supercomputers of the M3PEC-Mésocentre, belonging to the University Bordeaux 1 and partly financed by the Conseil Régional d'Aquitaine and the French Ministry of Research and Technology (MRNT). B.C., E.G., and R.P. are indebted to EGIDE and DAAD for research grants within the PROCOPE programs (Grants 17841TJ and D/0707570). This work was supported by the Deutsche Forschungsgemeinschaft through SPP 1458 Hochtemperatursupraleitung in Eisenpnictiden.